

Brown Carbon Aerosol in Urban Xi'an, Northwest China: The Composition and Light Absorption Properties

Ru-Jin Huang,^{*,†} Lu Yang,[†] Junji Cao,[†] Yang Chen,[‡] Qi Chen,[§] Yongjie Li,[⊥] Jing Duan,[†] Chongshu Zhu,[†] Wenting Dai,[†] Kai Wang,^{†,¶} Chunshui Lin,^{†,○} Haiyan Ni,^{†,◆} Joel C. Corbin,[#] Yunfei Wu,[▽] Renjian Zhang,[▽] Xuexi Tie,[†] Thorsten Hoffmann,[¶] Colin O'Dowd,[○] and Uli Dusek[◆]

[†]Key Laboratory of Aerosol Chemistry and Physics, State Key Laboratory of Loess and Quaternary Geology, Institute of Earth and Environment, Chinese Academy of Sciences, Xi'an 710061, China

[‡]Chongqing Institute of Green and Intelligent Technology, Chinese Academy of Sciences, Chongqing 400714, China

[§]State Key Joint Laboratory of Environmental Simulation and Pollution Control, College of Environmental Sciences and Engineering, Peking University, Beijing 100871, China

[⊥]Department of Civil and Environmental Engineering, Faculty of Science and Technology, University of Macau, Taipa 000000, Macau China

[¶]Institute of Inorganic and Analytical Chemistry, Johannes Gutenberg University of Mainz, Duesbergweg 10–14, Mainz 55128, Germany

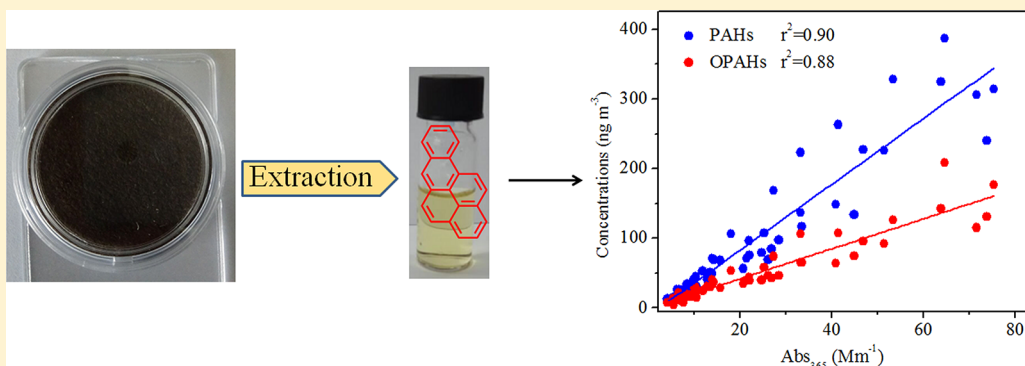
[○]School of Physics and Centre for Climate and Air Pollution Studies, Ryan Institute, National University of Ireland Galway, University Road, Galway H91CF50, Ireland

[▽]RCE-TEA, Institute of Atmospheric Physics, Chinese Academy of Sciences, Beijing 100029, China

[#]Laboratory of Atmospheric Chemistry, Paul Scherrer Institute (PSI), Villigen 5232, Switzerland

[◆]Centre for Isotope Research (CIO), Energy and Sustainability Research Institute Groningen (ESRIG), University of Groningen, Groningen 9747 AG The Netherlands

Supporting Information



ABSTRACT: Light-absorbing organic carbon (i.e., brown carbon or BrC) in the atmospheric aerosol has significant contribution to light absorption and radiative forcing. However, the link between BrC optical properties and chemical composition remains poorly constrained. In this study, we combine spectrophotometric measurements and chemical analyses of BrC samples collected from July 2008 to June 2009 in urban Xi'an, Northwest China. Elevated BrC was observed in winter (5 times higher than in summer), largely due to increased emissions from wintertime domestic biomass burning. The light absorption coefficient of methanol-soluble BrC at 365 nm (on average approximately twice that of water-soluble BrC) was found to correlate strongly with both parent polycyclic aromatic hydrocarbons (parent-PAHs, 27 species) and their carbonyl oxygenated derivatives (carbonyl-OPAHs, 15 species) in all seasons ($r^2 > 0.61$). These measured parent-PAHs and carbonyl-OPAHs account for on average $\sim 1.7\%$ of the overall absorption of methanol-soluble BrC, about 5 times higher than their mass fraction in total organic carbon (OC, $\sim 0.35\%$). The fractional solar absorption by BrC relative to element carbon (EC) in the ultraviolet range (300–400 nm) is significant during winter ($42 \pm 18\%$ for water-soluble BrC and $76 \pm 29\%$ for methanol-soluble BrC), which may greatly affect the radiative balance and tropospheric photochemistry and therefore the climate and air quality.

INTRODUCTION

Carbonaceous aerosol, including organic carbon (OC) and black carbon (BC), constitutes a large fraction of atmospheric aerosol

Received: May 4, 2018

Accepted: May 25, 2018

Published: May 25, 2018

and influences Earth's climate directly by absorbing and scattering radiation. The importance of BC has been well documented over the past decades because of its strong light absorption coefficient.^{1–4} However, only in recent years has the role of brown carbon (BrC) been recognized.^{5–16} BrC is a group of light absorbing organic compounds with absorption increasing sharply from the visible (Vis) to ultraviolet (UV) range. Although the mass absorption efficiency of BrC is lower than that of BC, its contribution to the UV absorption of carbonaceous aerosol is potentially significant due to the much higher abundance of OC compared to BC in continental aerosol. In addition to the direct effect on solar radiation, BrC immersed in cloud droplets absorbs light and might facilitate water evaporation and cloud dispersion, which is an additional indirect effect that counteracts the cooling effect of cloud droplet nucleation by aerosol.¹⁷

The sources of BrC are not well characterized so far. Emissions from incomplete and smoldering combustion of biomass, including forest fires, burning of wood and agricultural waste, are known to be a main source of BrC.^{18–22} Coal combustion is also recognized to be the source of BrC, particularly in areas with residential coal combustion.^{23–25} BrC can also be produced from atmospheric processes other than direct combustion emissions. As summarized in a recent review paper,¹⁵ “secondary BrC” can be formed from atmospheric multiphase reactions between the gas-phase, particle-phase, and cloud droplet constituents. The difference in BrC emission sources together with the formation of secondary BrC result in the complexity in BrC chemical composition and absorption properties. Additional complications stem from the dynamic evolution of BrC in its physicochemical properties as a consequence of atmospheric aging, which can either enhance or reduce light absorption by BrC.^{26–29} It is therefore a challenging task to investigate the effect of the dynamically evolving BrC composition on its absorption properties.

Measurements of BrC absorption properties can be realized by spectrophotometric analysis of aerosol extracts. As solution extracts of aerosol do not contain BC or mineral dust, the light absorption of BrC contained in these extracts can be measured without interference of BC or mineral dust.³⁰ Spectrophotometric analysis of solution extracts can also provide highly spectrally resolved data over a wide wavelength range. Further, chemical analysis of individual chromophores in the solution extracts and their correlation with spectrophotometric measurements can provide a better understanding of the effects of BrC molecular composition and chemistry on its optical properties. Such correlation studies are still in their early stages but are of importance because recent evidence shows that the overall absorption properties of some BrC compounds may be determined by the very minor presence of highly absorbing chromophores with unique molecular structures and precursor-specific chemistry in their formation and evolution.^{15,31}

Model studies show elevated BrC annual burden in the areas with large biomass burning activities, such as in Africa, India, and China.^{32,33} High concentrations of BrC in China may greatly influence the visibility, air quality, climate, and the tropospheric photochemistry. However, BrC related studies are still very scarce in China, with very limited studies focusing on the light absorption properties in megacities, for example, Beijing.^{34–36} Here, we extended the BrC studies to Xi'an, a megacity in northwest China experiencing severe particulate air pollution, especially in the wintertime domestic heating season due to enhanced biomass burning activities. The objectives of this study were to investigate (1) the concentrations and seasonal variations of BrC in urban Xi'an; (2) the correlation of BrC absorption with individual

chromophores; and (3) the fractional solar absorption by BrC relative to EC.

EXPERIMENTAL SECTION

Ambient Sample Collection. 24-h integrated PM_{2.5} samples were collected every 6 days on prebaked (780 °C, 3 h) quartz-fiber filters (8 × 10 in., Whatman, QM-A) using a Hi-Vol PM_{2.5} air sampler (Tisch, Cleveland, OH) at a flow rate of 1.05 m³ min⁻¹ from 5 July 2008 to 27 June 2009. After collection, the filter samples were immediately wrapped in baked aluminum foils and stored in a freezer (below -10 °C) until analysis. The sampling site was located on the rooftop of the Institute of Earth and Environment (~10 m above the ground), Chinese Academy of Sciences (IEECAS), which was surrounded by residential, commercial and traffic area (see Supporting Information (SI) Figure S1). The seasonal division was made according to the meteorological characteristics, that is, the period from 15 November to 14 March was designated as winter, from 15 March to 31 May as spring, from 1 June to 31 August as summer and from 1 September to 14 November as Fall.³⁷ SI Figure S2 show the seasonal frequency distribution of wind speed and wind direction.

Filter Extraction and Absorption Spectra Analysis. A portion of filter (0.526 cm² punch) taken from each sample was sonicated for 1 h in 10 mL of ultrapure water (>18.2 MΩ) or methanol (J. T. Baker, HPLC grade). The extracts were then filtered with a 0.45 μm PTFE pore syringe filter to remove insoluble material. The extraction efficiencies were tested by analyzing the absorption (365 nm) of the second extracts of the same filters and the OC remained on the filter after the first extraction (see SI and Figure S3). Absorption spectra of the extracts (water or methanol) were measured using a Liquid Waveguide Capillary Cell (LWCC-3100, World Precision Instrument) equipped with a UV-vis spectrophotometer (300–700 nm), following the method established by Hecobian et al. (2010).⁸ The extracts were diluted to the range where the Beer-Lambert law is valid before absorption spectra measurements. The spectra recorded were corrected for the filter blanks. The absorption data were converted to the absorption coefficient following eq 1

$$\text{Abs}_\lambda = (A_\lambda - A_{700}) \frac{V_l}{V_a \times l} \times \ln(10) \quad (1)$$

where Abs_λ (Mm⁻¹) represents the absorption coefficient of filter extracts at wavelength of λ. A_λ (arbitrary unit) is the absorbance recorded. V_l (in mL) corresponds to the volume of solvent (water or methanol) used to extract the filter sample, and V_a (in m³) is the volume of the air sampled through the filter punch. The optical length (l) of LWCC used here is 0.94 m and ln(10) converts the log base-10 (recorded by UV-vis spectrophotometer) to natural logarithm to provide base-e absorption coefficient. To account for baseline shift that may occur during analysis, absorption at all wavelengths below 700 nm are referenced to that of 700 nm where there is no absorption for ambient aerosol extracts. The average absorption coefficient between 360 and 370 nm (Abs₃₆₅) is used to represent BrC absorption in order to avoid interferences from nonorganic compounds (e.g., nitrate) and to maintain consistency with previous reported results.

The mass absorption efficiency (MAE) of the filter extract at wavelength of λ can be described as

$$\text{MAE}_\lambda = \frac{\text{Abs}_\lambda}{M} \quad (2)$$

where M (μgC m⁻³) is the water-soluble organic carbon (WSOC) concentration for water extracts or methanol-soluble organic

carbon (MSOC) concentration for methanol extracts. Note that for methanol extracts the use of an organic solvent prohibits determining carbon mass and therefore the OC concentration measured by the thermal/optical carbon analyzer is used assuming OC is completely extracted by methanol. This assumption may lead to underestimate of the MAE of methanol extracted BrC, although previous studies show high OC extraction efficiencies by methanol (e.g., ~95% for biomass burning OC and ~85% for ambient OC in Beijing).^{36,38}

The wavelength dependence for light absorption by chromophores in solution can be characterized by a power law equation:

$$\text{Abs}_\lambda = K \cdot \lambda^{-\text{AAE}} \quad (3)$$

where K is a constant related to chromophores concentration and AAE is termed the absorption Ångström exponent, which depends on the types of the chromophores in solution. The AAE of filter extracts is calculated by a linear regression of $\log \text{Abs}_\lambda$ versus $\log \lambda$ in the wavelength range of 330–550 nm. This range is chosen to (1) avoid interferences from nonorganic compounds at lower wavelength; (2) ensure sufficient signal-noise ratio for the investigate samples.

Chemical Analysis. OC and EC were measured by a DRI Model 2001 thermal/optical carbon analyzer following the IMPROVE-A temperature protocol. More details were described in previous studies.^{39,40} WSOC concentration was determined by a TOC/TN analyzer (TOC–L, Shimadzu, Japan) and details were described elsewhere.⁴¹ The concentrations of levoglucosan and water-soluble inorganic ions (NH_4^+ , SO_4^{2-} , NO_3^- , Cl^- , Na^+ , K^+ , Ca^{2+} , Mg^{2+}) were determined with ion chromatography following procedures described by Zhang et al.³⁷ The concentrations of particulate polycyclic aromatic hydrocarbons (PAHs) and their oxygenated (OPAHs) and nitro derivatives, including 27 parent-PAHs, 15 carbonyl-OPAHs, 8 hydroxyl- and carboxyl-OPAHs, and 9 nitro-PAHs, were analyzed with a gas chromatography–mass spectrometer (GC–MS) following methods described by Wang et al.⁴²

Direct Solar Absorption of Brown Carbon Relative to Element Carbon. The measurement of EC light absorption coefficient by thermal/optical carbon analyzer is similar to the determination of BC light absorption by Aethalometer, which measure the light attenuation through a particle-loaded and a particle-free reference quartz filter. Intercomparison between attenuation coefficient derived by the carbon analyzer and Aethalometer showed good agreement, indicating the equivalence of light absorption measurement by the two analytical methods.⁴³ The artifacts associated with the filter-based measurement of EC absorption coefficient were corrected following the method of Ram and Sarin⁴³ (see SI for more details). The direct solar absorption of brown carbon relative to EC was estimated by the approach similar to Kirchstetter and Thatcher⁴⁴ and Kirillova et al.⁴⁵ Briefly, light absorption by absorbing species x (BrC or EC herein) follows the Beer–Lambert's law as

$$\frac{I_0 - I}{I_0}(\lambda) = 1 - e^{-b_{\text{ap},x,\lambda} \cdot h_{\text{ABL}}} \quad (4)$$

where h_{ABL} corresponds to the boundary layer height (assuming 1000 m), $b_{\text{ap},x,\lambda}$ for EC denotes the absorption coefficient derived from the thermal/optical carbon analysis described above, and for BrC $b_{\text{ap},x,\lambda}$ represents the absorption coefficient of particulate BrC. Previous studies reported that the light absorption coefficient of particulate BrC is about 0.7–2.0 times that of BrC aerosol extract.^{46,47} Here, a conversion factor of 1 is applied

and the uncertainties are estimated. Then, the fraction of solar radiation absorbed by water- or methanol-soluble BrC aerosol relative to EC is given by

$$f = \frac{\int I_0(\lambda) \{1 - e^{-b_{\text{ap}, \text{BrC}(\text{water/methanol}), \lambda} \cdot h_{\text{ABL}}}\} d\lambda}{\int I_0(\lambda) \{1 - e^{-b_{\text{ap}, \text{EC}, \lambda} \cdot h_{\text{ABL}}}\} d\lambda} \quad (5)$$

where $I_0(\lambda)$ is the clear sky Air Mass 1 Global Horizontal solar irradiance.⁴⁸ The fraction f is obtained by numerical integration of the above formula in the wavelength range of 300–2500 nm, 300–700 nm and 300–400 nm for each sample, respectively. This approximate estimation is based on the following assumptions (1) the ground measurement results represent the whole atmospheric boundary layer; (2) the light absorption coefficient of BrC aerosol extract is equal to that of particulate BrC.

RESULTS AND DISCUSSION

Light Absorption Properties of Soluble BrC. Figure 1 shows the seasonal average absorption spectra of WSOC and MSOC at the wavelengths between 300 and 700 nm, which exhibit the common characteristic of BrC with sharply increasing absorbance toward shorter wavelength and is obviously different from the absorption properties of BC which are only weakly wavelength dependent with an AAE close to 1. The seasonal average AAE of WSOC varies slightly between 5.7 and 6.1 with mean values of 5.9, within the range of previous studies in, for example, the New Delhi, Beijing and outflow from northern China.^{35,45,49} The AAE of MSOC (6.0 ± 0.2) is comparable with that of WSOC, consistent with a previous study in urban Beijing during winter.³⁶ This feature is different from measurements in the Los Angeles Basin and the North American continental troposphere where the AAE values of MSOC are lower compared to AAE values of WSOC.^{13,50} The difference in AAE between China and North America might reflect the difference in emission sources and atmospheric processes which determine the composition of BrC chromophores. Another evident feature of BrC absorption spectra shown in Figure 1 is that absorption coefficient of MSOC is always greater than that of WSOC across all measurement wavelengths, which is consistent with previous studies. This can be attributed to the difference in type and amount of chromophores extracted, i.e., more chromophores are extracted in methanol (e.g., PAHs from biomass burning and fossil fuel combustion) but not in water.^{38,50} It should be noted that the change of pH from particles to water extracts may affect BrC absorption, as Phillips et al.⁵¹ showed that the BrC absorption increases by 10% per pH unit from pH 2–12. We calculated the particle pH value of the NH_4^+ - SO_4^{2-} - NO_3^- - Cl^- - Na^+ - K^+ - Ca^{2+} - Mg^{2+} system using the thermodynamic model ISORROPIA-II which was run in “forward” mode.⁵² Our results show that the average particle pH during the entire measurement period was 5.97, similar to previous studies in Xi'an.⁵³ Therefore, the pH change from particle to water extracts is likely less than 1 pH unit and the effect on BrC absorption is less than 10%.

Figure 2a and b show the time series of absorption coefficient of WSOC and MSOC at 365 nm (i.e., $\text{Abs}_{365, \text{WSOC}}$ and $\text{Abs}_{365, \text{MSOC}}$) as well as the concentrations of WSOC, OC, levoglucosan, parent-PAHs and carbonyl-OPAHs. They all show clear seasonal variations with enhanced values in winter. The seasonal averages for all measured parameters peak in winter, decreasing in fall and spring and reaching the minimum in summer (see SI Table S1). It should be noted that $\text{Abs}_{365, \text{MSOC}}$ is approximately two times (1.7–2.1) higher than $\text{Abs}_{365, \text{WSOC}}$ in all seasons, indicating that MSOC provides a better estimation of BrC than WSOC. Figure 2c shows

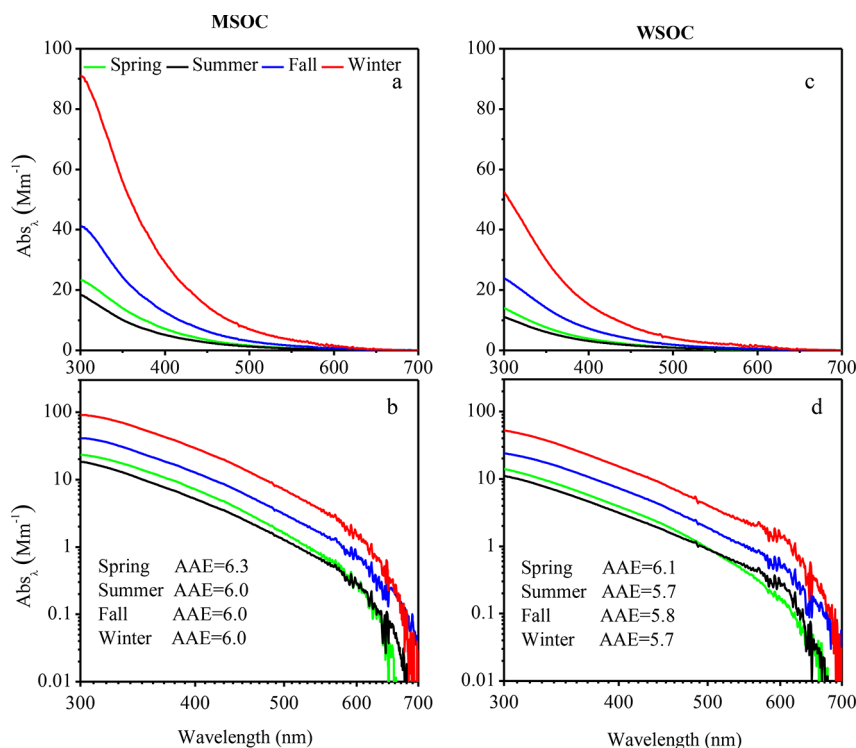


Figure 1. Seasonal average absorption spectra of MSOC (a and b) and WSOC (c and d) plotted on a linear (top) and logarithmic (bottom) scale. AAE is determined by a linear regression of $\log(\text{Abs}_\lambda)$ versus $\log(\lambda)$ in the wavelength range of 330–550 nm.

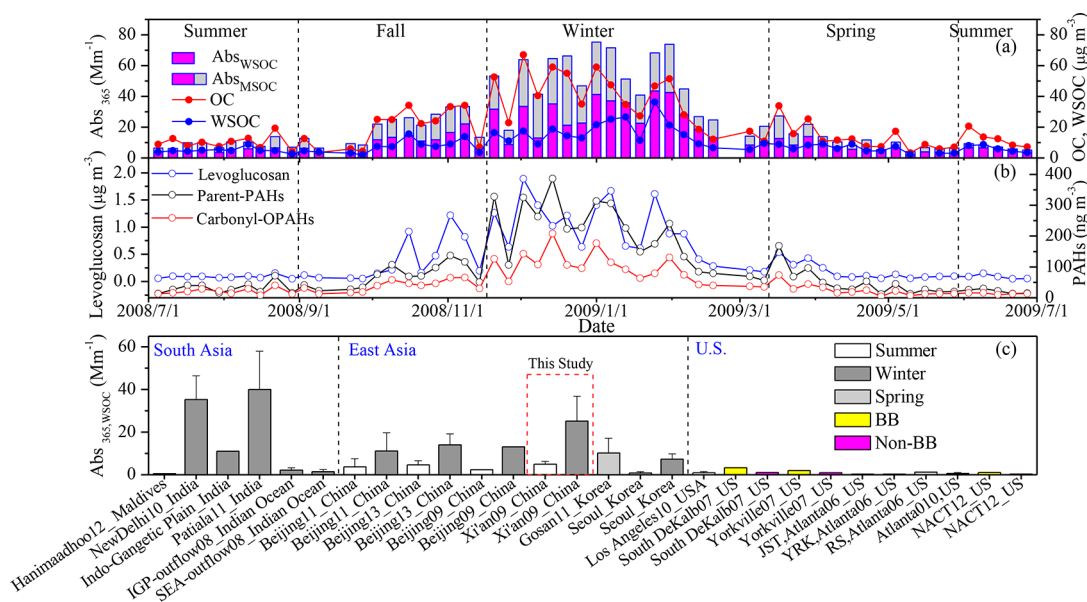


Figure 2. Time series of the light absorption coefficient of WSOC and MSOC at 365 nm ($\text{Abs}_{365,\text{WSOC}}$ and $\text{Abs}_{365,\text{MSOC}}$ respectively) as well as OC, WSOC (a) and levoglucosan, parent-PAHs, carbonyl-OPAHs concentrations (b) and comparison of $\text{Abs}_{365,\text{WSOC}}$ in South Asia, East Asia, and the United States (c).

the comparison with previous studies in East Asia, South Asia, and the U.S. Note that $\text{Abs}_{365,\text{MSOC}}$ was not measured in most previous studies and therefore only $\text{Abs}_{365,\text{WSOC}}$ values are compared here. It can be seen from the figure that $\text{Abs}_{365,\text{WSOC}}$ in the urban regions of South Asia and East Asia is much higher than that in the U.S., indicating the large difference in the composition and concentration of chromophores. The wintertime $\text{Abs}_{365,\text{WSOC}}$ is significantly higher than the summertime $\text{Abs}_{365,\text{WSOC}}$ in China ($P < 0.001$), which could be attributed

to the enhanced emissions of BrC from residential heating in winter.

Figure 3a and b show the correlation between $\text{Abs}_{365,\text{WSOC}}$ and WSOC and between $\text{Abs}_{365,\text{MSOC}}$ and OC, respectively. The slopes represent the seasonal average of mass absorption efficiency at the wavelength of 365 nm (MAE_{365}), which follows the descending order of winter > fall > spring > summer for both WSOC and MSOC (see also SI Table S1). The seasonal difference in $\text{MAE}_{365,\text{WSOC}}$ and $\text{MAE}_{365,\text{MSOC}}$ indicates the seasonal difference

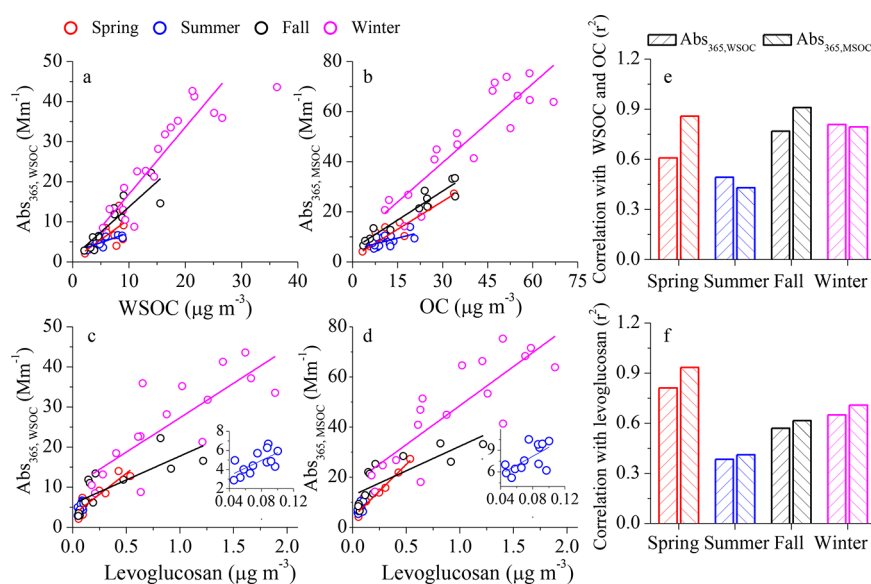


Figure 3. Scatter plots of Abs_{365,WSOC} and Abs_{365,MSOC} against WSOC and OC (a and b) and levoglucosan concentrations (c and d) and the corresponding linear correlation coefficients (e and f).

in the chemical composition and sources of BrC, the latter is further supported by the seasonal difference in correlation coefficient (r^2) of the linear regression. For example, a high correlation was observed in winter for both WSOC ($r^2=0.81$) and MSOC ($r^2 = 0.79$), which is consistent with the high correlation between Abs_{365,WSOC} and levoglucosan ($r^2 = 0.65$) and between Abs_{365,MSOC} and levoglucosan ($r^2 = 0.71$) in winter (Figure 3c and d), indicating that biomass burning emissions are the major source contributing to the absorption of BrC at Xi'an in winter (Biomass burning was found to be the dominant source of organic aerosol in Xi'an during winter^{37,54}). Furthermore, the MAE values (average of 1.65 for WSOC and 1.33 for MSOC) in winter are within the range of MAE of biomass burning (e.g., 1.3–1.8 for corn stalk,⁵⁵ 1.37 for rice straw,⁵⁶ ~ 1.9 for BB smoke particles⁵⁷), which further supports that biomass burning is the major BrC source in winter in Xi'an. In contrast to the wintertime case, a lower correlation was observed in summer for both WSOC ($r^2 = 0.49$) and MSOC ($r^2 = 0.31$) because more WSOC and MSOC in summer are derived from secondary organic aerosol (SOA) and many low molecular weight SOA compounds are colorless. The diversity in the sources of BrC in different seasons is further supported by the descending order of spring > winter > fall > summer for the correlation coefficient between Abs_{365,WSOC} and levoglucosan and between Abs_{365,MSOC} and levoglucosan (Figure 3c and d), and by the smaller correlation coefficient (except spring) between Abs_{365,WSOC} and levoglucosan and between Abs_{365,MSOC} and levoglucosan when compared to the corresponding correlation coefficient between Abs_{365,WSOC} and WSOC and between Abs_{365,MSOC} and OC. In other words, there existed other sources contributing to BrC in Xi'an in all seasons, particularly in summer (e.g., secondary BrC). Note that the high correlation suggests similar sources and lifetimes in the atmosphere and are not likely to be driven by changes in the boundary layer mixing volumes which are more like to promote changes in absolute concentration by a factor of ~2 as we observed in Xi'an between winter and summer (The boundary layer heights were 600–700 m in winter and 1300–1500 m in summer, respectively⁵⁸).

PAHs: An Efficient BrC Chromophore. PAHs are ubiquitous in atmospheric particles from incomplete combustion of biomass and coal. Data available in the literature show that some

PAHs, due to the large conjugated polycyclic structure, are strongly light-absorbing compounds at near-UV wavelength range (i.e., 300–400 nm, also see SI Figure S4) and therefore have been suggested to be important BrC chromophores.^{47,59,60}

In order to understand the potential contribution of PAHs to BrC absorption, the relationships between light absorption of BrC and the concentrations of parent-PAHs and carbonyl-OPAHs are examined. Scatter plots of parent-PAHs and carbonyl-OPAHs against Abs_{365,WSOC} and Abs_{365,MSOC} are shown in Figure 4. In general, parent-PAHs and carbonyl-OPAHs are correlated well with Abs_{365,MSOC} in all seasons ($r^2 > 0.61$). This result indicates that a significant part of BrC comes from a similar source as PAHs (i.e., incomplete combustion of biofuel or fossil fuel), or that PAHs are a significant fraction of BrC chromophores. Correlations of Abs_{365,WSOC} with parent-PAHs and carbonyl-OPAHs are lower compared to corresponding correlations with Abs_{365,MSOC} in all seasons. This is reasonable because parent-PAHs and carbonyl-OPAHs are organic solvent extractable (e.g., methanol) but mostly insoluble in water. Therefore, they contribute to methanol-soluble but not to water-soluble BrC absorption. The moderate correlation coefficient of Abs_{365,WSOC} with parent-PAHs and carbonyl-OPAHs may be ascribed to the water-soluble chromophores that coemitted with parent-PAHs and carbonyl-OPAHs from sources such as biomass burning and coal combustion. Again the extremely low correlations between Abs_{365,WSOC} and parent-PAHs and carbonyl-OPAHs in summer indicate that extra sources, not associated with PAHs (e.g., SOA), contribute to the light absorption of WSOC.

The potential contribution of PAHs to the bulk light absorption of BrC (300–700 nm) in ambient air is estimated following a method modified from Samburova et al.⁶⁰ who estimated the contribution of PAHs to BrC light absorption in biomass burning source emission. Here, the contribution was calculated based on two parameters: ambient mass concentrations of individual PAHs and its solar-spectrum-weighted light absorption efficiency—MAE_{PAH,av}. The latter was obtained by multiplying MAE of individual PAHs with the power distribution of the solar spectrum and spectrally integrated (see SI and Figure S5).⁵⁶ SI Table S2 summarizes the MAE_{PAH,av} of individual parent-PAHs and carbonyl-OPAHs studied here. The PAHs with

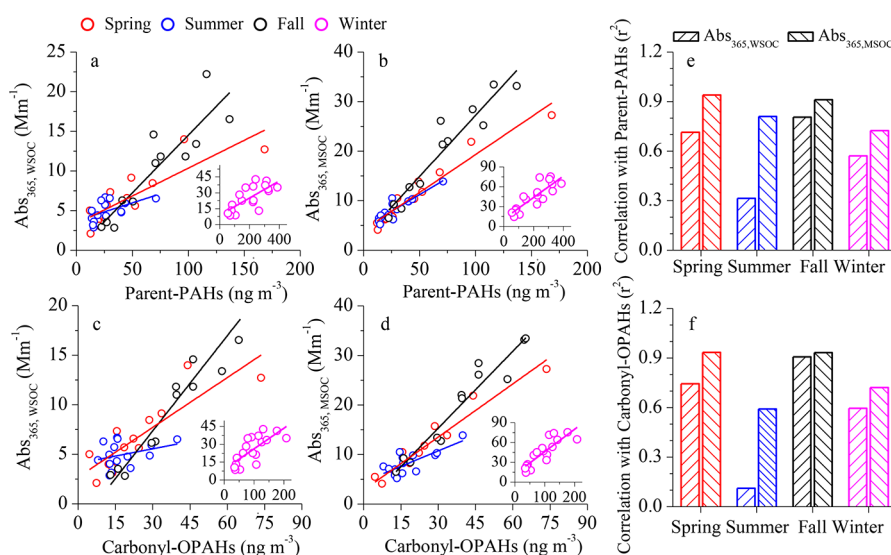


Figure 4. Scatter plots of $Abs_{365,WSOC}$ and $Abs_{365,MSOC}$ versus concentrations of parent-PAHs (a and b) and carbonyl-OPAHS (c and d) and the corresponding linear correlation coefficients (e and f).

Table 1. Annual Mean Contributions of Main BrC_PAHs Species to Methanol Extracted BrC Light Absorption

compounds	r^2 (conc.Vs $Abs_{365,MSOC}$)	$MAE_{PAH,av}^a$ ($m^2 g^{-1}$)	concentration ($ng m^{-3}$)	contribution to BrC light absorption (%)
indeno[1,2,3-cd]pyrene	0.804	1.0711	6.17	0.272
benzo[b+j+k]fluoranthenes	0.862	0.3475	18.04	0.244
benzo[a]pyrene	0.807	0.7709	8.6	0.241
benzo[e]pyrene	0.863	0.7709	7.94	0.240
pyrene	0.849	0.3530	7.97	0.082
perylene	0.787	1.7942	1.09	0.074
coronene	0.777	0.2774	6.93	0.073
benzo[ghi]perylene	0.759	0.1821	6.64	0.052
retene	0.736	0.1969	10.12	0.044
benzo[a]anthracene	0.786	0.2842	4.81	0.041
fluoranthene	0.867	0.2834	3.52	0.028
dibenzo[a,h]anthracene	0.840	0.2842	1.33	0.015
chrysene	0.887	0.0883	4.99	0.014
anthracene	0.788	0.2801	0.65	0.006
7H-Benz[de]anthracene-7-one	0.796	0.4385	9.01	0.138
5,12-naphthacenedione	0.773	0.3069	2.76	0.026
9,10-anthracenedione	0.864	0.1033	5.26	0.015
9-fluorenone	0.847	0.0920	1.79	0.083
total				1.688

^a $MAE_{PAH,av}$ of individual PAH is obtained by multiplying MAE of individual PAHs with the power distribution of the solar spectrum and spectrally integrated (see Supporting Information).

$MAE_{PAH,av} > 0.1 m^2 g^{-1}$ are named BrC_PAHs, which have strong light absorption properties in the blue and near-UV spectral region. Individual BrC_PAHs shows good correlation with $Abs_{365,MSOC}$ ($r^2 > 0.73$, see Table 1), indicating further that these PAHs are likely a significant fraction of BrC chromophores. The contributions of individual BrC_PAHs to the BrC bulk light absorption (300–700 nm) are estimated by dividing solar-spectrum-weighted absorption coefficient of MSOC by that of BrC_PAHs ($MAE_{PAH,av} \times PAH$ concentration). The overall annual average contribution of all BrC_PAHs listed in Table 1 to the BrC bulk light absorption is about 1.7%. This contribution is about 5 times of their mass contribution to organic carbon ($\sim 0.35\%$), indicating that even small amounts of light-absorbing compounds can have a disproportionately high impact on the light absorption properties of BrC. Besides PAHs, a few compounds have been identified as BrC chromophore. Laboratory study

showed that N-heterocyclic PAHs (N-PAHs) with 4–6 aromatic rings emitted from biomass burning are likely important BrC chromophores but they absorb more solar radiation in the visible wavelength range (400–500 nm) than their corresponding PAHs.⁶¹ Mohr et al.⁶² quantified five nitrated phenol compounds which accounted for $\sim 4\%$ of BrC light absorption at 370 nm in ambient air in Detling, United Kingdom. Zhang et al.⁵⁰ identified eight nitro-aromatic compounds in aerosol extracts in Los Angeles Basin, which contributed to $\sim 4\%$ of water-soluble BrC light absorption at 365 nm. Teich et al.⁶³ determined eight nitrated aromatic compounds in aerosol samples collected in Germany and China. The mean contribution of these nitrated aromatic compounds to water-soluble BrC light absorption at 370 nm ranged from 0.1 to 1.3% under acidic condition and from 0.1 to 3.7% under alkaline condition. However, in cloudwater samples heavily affected by biomass burning collected at Mount Tai,

Table 2. Average Direct Solar Absorbance of BrC Relative to EC during Summer and Winter

	WSOC/EC			MSOC/EC		
	$f_{300-2500}$ nm (%)	$f_{300-700}$ nm (%)	$f_{300-400}$ nm (%)	$f_{300-2500}$ nm (%)	$f_{300-700}$ nm (%)	$f_{300-400}$ nm (%)
summer	2 ± 1	3 ± 1	9 ± 3	4 ± 1	5 ± 1	15 ± 3
winter	10 ± 4	15 ± 6	42 ± 18	18 ± 7	26 ± 10	76 ± 29

Desyaterik et al.⁶⁴ identified 16 major light-absorbing compounds (mainly nitrophenols and aromatic carbonyls compounds), which contributed to ~50% of BrC light absorption between 300 and 400 nm. In general, a large fraction of BrC chromophores are still not identified so far. More studies are therefore necessary to better understand the link between BrC light absorption properties and the chemical composition.

Direct Solar Absorption of Brown Carbon Relative to Element Carbon. The importance of BrC optical properties is evaluated by calculating the fractional solar absorption by BrC relative to EC following eq 5 and the results are shown in Table 2. In the whole range of solar spectrum (300–2500 nm), the amount of solar radiation absorbed by WSOC relative to EC is only 2 ± 1% and 10 ± 4% in summer and winter, respectively, which are similar to previous studies in Beijing (6 ± 3% in summer and 11 ± 3% in winter),³⁵ New Delhi (6 ± 3% in winter)⁴⁵ and Gosan, Korea (6 ± 2% in winter).⁴⁹ MOSC shows slightly higher contribution (i.e., 3 ± 1% in summer and 18 ± 7% in winter). However, when considering the UV range (300–400 nm) only, the fractional solar absorption by WSOC relative to EC increases to 9 ± 3% in summer and to 42 ± 18% in winter. The contribution from MSOC increases further to 15 ± 3% in summer and to 76 ± 29% in winter. It should be noted that these calculated results provide an approximate estimate of the relative climate effect of BrC relative to EC, which may be affected by the uncertainties associated with the assumptions (i.e., AAE of EC (AAE_{EC}) is set to 1 and the light absorption coefficient of particulate BrC is equal to that of BrC aerosol extract). When the upper limit value of AAE_{EC} (1.4) is applied, the fractional solar absorption by BrC relative to EC in the UV range is still significant (38 ± 16% for WSOC and 68 ± 26% for MSOC during winter) (see SI Table S3). Likewise, direct solar absorption of BrC relative to EC is significant when the conversion factor of light absorption coefficient between BrC aerosol extract and particulate BrC varies from 0.7 to 2.0 (see SI Table S4), although this estimate has its limitations derived from the simplifying assumptions, for example, the light absorption of aerosol extracts may not be directly translated into the absorption of ambient aerosol considering the size distribution of aerosol, the effects of internal mixing and the changes in absorption caused by dissolving the chromophores into methanol or water. Note that although a constant boundary layer height of 1000 m was used for the calculation, uncertainty analysis indicates that the change of boundary layer height from 500 to 1500 m has a minor effect on the results (<2%). These results indicate that although EC is the main light-absorbing carbonaceous species in the atmosphere, the effect of BrC should not be ignored, especially in the lower wavelength (i.e., below 400 nm) during winter season. In general, the strong absorption of solar radiation by BrC in the UV range may significantly affect the radiative balance and therefore the tropospheric photochemistry. For example, Jo et al.⁶⁵ estimated that the inclusion of BrC absorption (traditional scattering only) can lead to the decrease of annual NO₂ photolysis rate by up to ~8% in surface air over Asia and therefore 6% reduction of annual mean surface O₃ concentration. Hammer et al.⁶⁶ examined the effects of BrC absorption on the tropospheric

OH photochemistry and found that OH concentrations decreased by ~5% over China in April 2007 due to BrC absorption. Therefore, future climate and air quality model should consider the effect of BrC absorption.

Despite the uncertainties derived from assumptions discussed above, our results show the significance of the direct solar absorption of BrC relative to EC. Understanding the BrC sources, molecular composition and chemistry as well as the links with optical properties are critical for better quantifying the implications of BrC, but is still in its early stages as discussed in a recent review paper.¹⁵ Similar to nitrated phenols, nitrated aromatics,^{50,62,63} the PAHs and carbonyl-OPAHs quantified here also only explain a small fraction of BrC light absorption but their concentrations are strongly correlated with MSOC absorption. Future studies of BrC chemical characterization should target the speciation of compounds coemitted with PAHs or the identification of common features (e.g., functional groups) and proxy compounds.

■ ASSOCIATED CONTENT

📄 Supporting Information

The Supporting Information is available free of charge on the ACS Publications website at DOI: 10.1021/acs.est.8b02386.

Tables S1–S4 and Figures S1–S5 with addition experimental procedures and results as described in the text (PDF)

■ AUTHOR INFORMATION

Corresponding Author

*E-mail: rujin.huang@ieecas.cn.

ORCID

Chunshui Lin: 0000-0003-3175-6778

Notes

The authors declare no competing financial interest.

■ ACKNOWLEDGMENTS

This work was supported by the National Natural Science Foundation of China (NSFC) under Grant No. 91644219, No. 41673134, and No. 41650110488. We also acknowledge the grant KNAW (No. 530-SCDP30) from The Netherlands.

■ REFERENCES

- (1) Jacobson, M. Z. Strong radiative heating due to the mixing state of black carbon in atmospheric aerosols. *Nature* **2001**, *409*, 695–697.
- (2) Menon, S.; Hansen, J.; Nazarenko, L.; Luo, Y. F. Climate effects of black carbon aerosols in China and India. *Science* **2002**, *297*, 2250–2253.
- (3) Derimian, Y.; Karnieli, A.; Kaufman, Y. J.; Andreae, M. O.; Andreae, T. W.; Dubovik, O.; Maenhut, W.; Koren, I. The role of iron and black carbon in aerosol light absorption. *Atmos. Chem. Phys.* **2008**, *8*, 3623–3637.
- (4) Bond, T. C.; Doherty, S. J.; Fahey, D. W.; Forster, P. M.; Berntsen, T.; DeAngelo, B. J.; Flanner, M. G.; Ghan, S.; Kärcher, B.; Koch, D.; Kinne, S.; Kondo, Y.; Quinn, P. K.; et al. Bounding the role of black carbon in the climate system: A scientific assessment. *J. Geophys. Res.* **2013**, *118*, 5380–5552.

- (5) Andreae, M. O.; Gelencser, A. Black carbon or brown carbon? The nature of light-absorbing carbonaceous aerosols. *Atmos. Chem. Phys.* **2006**, *6*, 3131–3148.
- (6) Lukács, H.; Gelencser, A.; Hammer, S.; Puxbaum, H.; Pio, C.; Legrand, M.; Kasper-Giebl, A.; Handler, M.; Limbeck, A.; Simpson, D.; Preunkert, S. Seasonal trends and possible sources of brown carbon based on 2-year aerosol measurements at six sites in Europe. *J. Geophys. Res.* **2007**, *112*, D23S18.
- (7) Alexander, D. T. L.; Crozier, P. A.; Anderson, J. R. Brown carbon spheres in East Asian outflow and their optical properties. *Science* **2008**, *321*, 833–836.
- (8) Hecobian, A.; Zhang, X.; Zheng, M.; Frank, N. H.; Edgerton, E. S.; Weber, R. J. Water-soluble organic aerosol material and the light absorption characteristics of aqueous extracts measured over the Southeastern United States. *Atmos. Chem. Phys.* **2010**, *10*, 5965–5977.
- (9) Lack, D. A.; Cappa, C. D. Impact of brown and clear carbon on light absorption enhancement, single scatter albedo and absorption wavelength dependence of black carbon. *Atmos. Chem. Phys.* **2010**, *10*, 4207–4220.
- (10) Park, R. J.; Kim, M. J.; Jeong, J. I.; Youn, D.; Kim, S. A contribution of brown carbon aerosol to the aerosol light absorption and its radiative forcing in East Asia. *Atmos. Environ.* **2010**, *44*, 1414–1421.
- (11) Bahadur, R.; Praveen, P. S.; Xu, Y.; Ramanathan, V. Solar absorption by elemental and brown carbon determined from spectral observations. *Proc. Natl. Acad. Sci. U. S. A.* **2012**, *109*, 17366–17371.
- (12) IPCC. *Fifth Assessment Report: Climate Change 2013*; Cambridge University Press: New York, 2013.
- (13) Liu, J.; Scheuer, E.; Dibb, J.; Diskin, G. S.; Ziemba, L. D.; Thornhill, K. L.; Anderson, B. E.; Wisthaler, A.; Mikoviny, T.; Devi, J. J.; et al. Brown carbon aerosol in the North American continental troposphere: Sources, abundance, and radiative forcing. *Atmos. Chem. Phys.* **2015**, *15*, 7841–7858.
- (14) Washenfelder, R. A.; Attwood, A. R.; Brock, C. A.; Guo, H.; Xu, L.; Weber, R. J.; Ng, N. L.; Allen, H. M.; Ayres, B. R.; Baumann, K.; et al. Biomass burning dominates brown carbon absorption in the rural southeastern United States. *Geophys. Res. Lett.* **2015**, *42*, 653–664.
- (15) Laskin, A.; Laskin, J.; Nizkorodov, S. A. Chemistry of atmospheric brown carbon. *Chem. Rev.* **2015**, *115*, 4335–4382.
- (16) Costabile, F.; Gilardoni, S.; Barnaba, F.; Di Ianni, A.; Di Liberto, L.; Dionisi, D.; Manigrasso, M.; Paglione, M.; Poluzzi, V.; Rinaldi, M.; Facchini, M. C.; Gobbi, G. P. Characteristics of brown carbon in the urban Po Valley atmosphere. *Atmos. Chem. Phys.* **2017**, *17*, 313–326.
- (17) Hansen, J.; Sato, M.; Ruedy, R. J. *Geophys. Res.-Atmos* **1997**, *102*, 6831–6864.
- (18) Chakrabarty, R. K.; Moosmuller, H.; Chen, L. W. A.; Lewis, K.; Arnott, W. P.; Mazzoleni, C.; Dubey, M. K.; Wold, C. E.; Hao, W. M.; Kreidenweis, S. M. Brown carbon in tar balls from smoldering biomass combustion. *Atmos. Chem. Phys.* **2010**, *10*, 6363–6370.
- (19) Kirchstetter, T. W.; Thatcher, T. L. Contribution of organic carbon to wood smoke particulate matter absorption of solar radiation. *Atmos. Chem. Phys.* **2012**, *12*, 6067–6072.
- (20) Lack, D. A.; Langridge, J. M.; Bahreini, R.; Cappa, C. D.; Middlebrook, A. M.; Schwarz, J. P. Brown carbon and internal mixing in biomass burning particles. *Proc. Natl. Acad. Sci. U. S. A.* **2012**, *109*, 14802–14807.
- (21) Chakrabarty, R. K.; Pervez, S.; Chow, J. C.; Watson, J. G.; Dewangan, S.; Robles, J.; Tian, G. Funeral pyres in South Asia: brown carbon aerosol emissions and climate impacts. *Environ. Sci. Technol. Lett.* **2014**, *1*, 44–48.
- (22) Chakrabarty, R. K.; Gyawali, M.; Yatavelli, R. L. N.; Pandey, A.; Watts, A. C.; Knue, J.; Chen, L.-W. A.; Pattison, R. R.; Tsiabart, A.; Samburova, V.; Moosmüller, H. Brown carbon aerosols from burning of boreal peatlands: microphysical properties, emission factors, and implications for direct radiative forcing. *Atmos. Chem. Phys.* **2016**, *16*, 3033–3040.
- (23) Bond, T. C.; Covert, D. S.; Kramlich, J. C.; Larson, T. V.; Charlson, R. J. Primary particle emissions from residential coal burning: Optical properties and size distributions. *J. Geophys. Res.* **2002**, *107* (D21), 8347.
- (24) Yang, M.; Howell, S. G.; Zhuang, J.; Huebert, B. J. Attribution of aerosol light absorption to black carbon, brown carbon, and dust in China—interpretations of atmospheric measurements during EAST-AIRE. *Atmos. Chem. Phys.* **2009**, *9*, 2035–2050.
- (25) Sun, J. Z.; Zhi, G. R.; Hitznerberger, R.; Chen, Y. J.; Tian, C. G.; Zhang, Y. Y.; Feng, Y. L.; Cheng, M.; Zhang, Y. Z.; Cai, J.; Chen, F.; Qiu, Y. Q.; Jiang, Z. M.; Li, J.; Zhang, G.; Mo, Y. Z. Emission factors and light absorption properties of brown carbon from household coal combustion in China. *Atmos. Chem. Phys.* **2017**, *17*, 4769–4780.
- (26) Lambe, A. T.; Cappa, C. D.; Massoli, P.; Onasch, T. B.; Forestieri, S. D.; Martin, A. T.; Cummings, M. J.; Croasdale, D. R.; Brune, W. H.; Worsnop, D. R.; Davidovits, P. Relationship between oxidation level and optical properties of secondary organic aerosol. *Environ. Sci. Technol.* **2013**, *47*, 6349–6357.
- (27) Lee, H. J.; Aiona, P. K.; Laskin, A.; Laskin, J.; Nizkorodov, S. A. Effect of solar radiation on the optical properties and molecular composition of laboratory proxies of atmospheric brown carbon. *Environ. Sci. Technol.* **2014**, *48*, 10217–10226.
- (28) Zhong, M.; Jang, M. Dynamic light absorption of biomassburning organic carbon photochemically aged under natural sunlight. *Atmos. Chem. Phys.* **2014**, *14*, 1517–1525.
- (29) Updyke, K. M.; Nguyen, T. B.; Nizkorodov, S. A. Formation of brown carbon via reactions of ammonia with secondary organic aerosols from biogenic and anthropogenic precursors. *Atmos. Environ.* **2012**, *63*, 22–31.
- (30) Lack, D. A.; Langridge, J. M. On the attribution of black and brown carbon light absorption using the Angstrom exponent. *Atmos. Chem. Phys.* **2013**, *13*, 10535–10543.
- (31) Laskin, J.; Laskin, A.; Nizkorodov, S. A.; Roach, P.; Eckert, P.; Gilles, M. K.; Wang, B. B.; Lee, H. J.; Hu, Q. C. Molecular selectivity of brown carbon chromophores. *Environ. Sci. Technol.* **2014**, *48*, 12047–12055.
- (32) Arola, A.; Schuster, G.; Myhre, G.; Kazadzis, S.; Dey, S.; Tripathi, S. N. Inferring absorbing organic carbon content from AERONET data. *Atmos. Chem. Phys.* **2011**, *11*, 215–225.
- (33) Feng, Y.; Ramanathan, V.; Kotamarthi, V. R. Brown carbon: A significant atmospheric absorber of solar radiation? *Atmos. Chem. Phys.* **2013**, *13*, 8607–8621.
- (34) Du, Z. Y.; He, K. B.; Cheng, Y.; Duan, F. K.; Ma, Y. L.; Liu, J. M.; Zhang, X. L.; Zheng, M.; Weber, R. J. A yearlong study of water-soluble organic carbon in Beijing II: light absorption properties. *Atmos. Environ.* **2014**, *89*, 235–241.
- (35) Yan, C.; Zheng, M.; Sullivan, A. P.; Bosch, C.; Desyaterik, Y.; Andersson, A.; Li, X.; Guo, X.; Zhou, T.; Gustafsson, Ö.; Collett, J. L., Jr. Chemical characteristics and light absorbing property of water-soluble organic carbon in Beijing: Biomass burning contributions. *Atmos. Environ.* **2015**, *121*, 4–12.
- (36) Cheng, Y.; He, K. B.; Du, Z. Y.; Engling, G.; Liu, J. M.; Ma, Y. L.; Zheng, M.; Weber, R. J. The characteristics of brown carbon aerosol during winter in Beijing. *Atmos. Environ.* **2016**, *127*, 355–364.
- (37) Zhang, T.; Cao, J. J.; Chow, J. C.; Shen, Z. X.; Ho, K. F.; HO, H. S. S.; Liu, S. X.; Han, Y. M.; Watson, J. G.; Wang, G. H.; Huang, R. J. Characterization and seasonal variations of levoglucosan in fine particulate matter in Xi'an. *J. Air Waste Manage. Assoc.* **2014**, *64*, 1317–1327.
- (38) Chen, Y.; Bond, T. C. Light absorption by organic carbon from wood combustion. *Atmos. Chem. Phys.* **2010**, *10*, 1773–1787.
- (39) Cao, J. J.; Wu, F.; Chow, J. C.; Lee, S. C.; Li, Y.; Chen, S. W.; An, Z. S.; Fung, K. K.; Watson, J. G.; Zhu, C. S.; Liu, S. X. Characterization and source apportionment of atmospheric organic and elemental carbon during fall and winter of 2003 in Xi'an, China. *Atmos. Chem. Phys.* **2005**, *5*, 3127–3137.
- (40) Chow, J. C.; Watson, J. G.; Robles, J.; Wang, X. L.; Chen, L. W. A.; Trimble, D. L.; Kohl, S. D.; Tropp, R. J.; Fung, K. K. Quality assurance and quality control for thermal/optical analysis of aerosol samples for organic and elemental carbon. *Anal. Bioanal. Chem.* **2011**, *401*, 3141–3152.
- (41) Ho, K. F.; Ho, S. S. H.; Huang, R. J.; Liu, S. X.; Cao, J. J.; Zhang, T.; Chuang, H. C.; Chan, C. S.; Hu, D.; Tian, L. Characteristics of water-

soluble organic nitrogen in fine particulate matter in the continental area of China. *Atmos. Environ.* **2015**, *106*, 252–261.

(42) Wang, J. Z.; Xu, H. M.; Guinot, B.; Li, L. J.; Ho, S. S. H.; Liu, S. X.; Li, X. P.; Cao, J. J. Concentrations, sources and health effects of parent, oxygenated- and nitrated- polycyclic aromatic hydrocarbons (PAHs) in middle-school air in Xi'an, China. *Atmos. Res.* **2017**, *192*, 1–10.

(43) Ram, K.; Sarin, M. M. Absorption coefficient and site-specific mass absorption efficiency of elemental carbon in aerosols over urban, rural, and high-altitude sites in India. *Environ. Sci. Technol.* **2009**, *43*, 8233–8239.

(44) Kirchstetter, T. W.; Thatcher, T. L. Contribution of organic carbon to wood smoke particulate matter absorption of solar radiation. *Atmos. Chem. Phys.* **2012**, *12*, 6067–6072.

(45) Kirillova, E. N.; Andersson, A.; Tiwari, S.; Srivastava, A. K.; Bisht, S. D.; Gustafsson, Ö. Water-soluble organic carbon aerosols during a full New Delhi winter: Isotope-based source apportionment and optical properties. *J. Geophys. Res. Atmos.* **2014**, *119*, 3476–3485.

(46) Liu, J.; Bergin, M.; Guo, H.; King, L.; Kotra, N.; Edgerton, E.; Weber, R. J. Size-resolved measurements of brown carbon in water and methanol extracts and estimates of their contribution to ambient fine particle light absorption. *Atmos. Chem. Phys.* **2013**, *13*, 12389–12404.

(47) Sun, H.; Biedermann, L.; Bond, T. C. Color of brown carbon: A model for ultraviolet and visible light absorption by organic carbon aerosol. *Geophys. Res. Lett.* **2007**, *34*, L17813.

(48) Levinson, R.; Akbari, H.; Berdahl, P. Measuring solar reflectance—Part I: defining a metric that accurately predicts solar heat gain. *Sol. Energy* **2010**, *84*, 1717–1744.

(49) Kirillova, E. N.; Andersson, A.; Han, J.; Lee, M.; Gustafsson, Ö. Sources and light absorption of water-soluble organic carbon aerosols in the outflow from northern China. *Atmos. Chem. Phys.* **2014**, *14*, 1413–1422.

(50) Zhang, X. L.; Lin, Y. H.; Surratt, J. D.; Weber, R. J. Sources, composition and absorption angstrom exponent of light-absorbing organic components in aerosol extracts from the Los Angeles Basin. *Environ. Sci. Technol.* **2013**, *47*, 3685–3693.

(51) Phillips, S. M.; Bellcross, A. D.; Smith, G. D. Light absorption by brown carbon in the southeastern United States is pH-dependent. *Environ. Sci. Technol.* **2017**, *51*, 6782–6790.

(52) Fountoukis, C.; Nenes, A. ISORROPIA II: a computationally efficient thermodynamic equilibrium model for K^+ – Ca^{2+} – Mg^{2+} – NH_4^+ – Na^+ – SO_4^{2-} – NO_3^- – Cl^- – H_2O aerosols. *Atmos. Chem. Phys.* **2007**, *7*, 4639–4659.

(53) Wang, G. H.; Zhang, R. Y.; Gomez, M. E.; et al. Persistent sulfate formation from London Fog to Chinese haze. *Proc. Natl. Acad. Sci. U. S. A.* **2016**, *113*, 13630–13635.

(54) Elser, M.; Huang, R.-J.; Wolf, R.; Slowik, J. G.; Wang, Q.; Canonaco, F.; Li, G.; Bozzetti, C.; Daellenbach, K. R.; Huang, Y.; Zhang, R.; Li, Z.; Cao, J.; Baltensperger, U.; El-Haddad, I.; Prévôt, A. S. H. New insights into $PM_{2.5}$ chemical composition and sources in two major cities in China during extreme haze events using aerosol mass spectrometry. *Atmos. Chem. Phys.* **2016**, *16*, 3207–3225.

(55) Li, X.; Chen, Y.; Bond, T. C. Light absorption of organic aerosol from pyrolysis of corn stalk. *Atmos. Environ.* **2016**, *144*, 249–256.

(56) Park, S. S.; Yu, J. Chemical and light absorption properties of humic-like substances from biomass burning emissions under controlled combustion experiments. *Atmos. Environ.* **2016**, *136*, 114–122.

(57) Lin, P.; Bluvshstein, N.; Rudich, Y.; Nizkorodov, S.; Laskin, J.; Laskin, A. Molecular chemistry of atmospheric brown carbon inferred from a nationwide biomass burning event. *Environ. Sci. Technol.* **2017**, *51*, 11561–11570.

(58) Zhao, S. Y.; Tie, X. X.; Cao, J. J.; Li, N.; Li, G. H.; Zhang, Q.; Zhu, C. S.; Long, X.; Li, J. D.; Feng, T.; Su, X. L. Seasonal variation and four-year trend of black carbon in the mid-west China: The analysis of the ambient measurement and WRF-Chem modeling. *Atmos. Environ.* **2015**, *123*, 430–439.

(59) Jacobson, M. Z. Isolating nitrated and aromatic aerosols and nitrated aromatic gases as sources of ultraviolet light absorption. *J. Geophys. Res.* **1999**, *104*, 3527–3542.

(60) Samburova, V.; Connolly, J.; Gyawali, M.; Yatavelli, R. L. N.; Watts, A. C.; Chakrabarty, R. K.; Zielinska, B.; Moosmüller, H.; Khlystov, A. Polycyclic aromatic hydrocarbons in biomass-burning emissions and their contribution to light absorption and aerosol toxicity. *Sci. Total Environ.* **2016**, *568*, 391–401.

(61) Lin, P.; Aiona, P. K.; Li, Y.; Shiraiwa, M.; Laskin, J.; Nizkorodov, S. A.; Laskin, A. Molecular characterization of brown carbon in biomass burning aerosol particles. *Environ. Sci. Technol.* **2016**, *50*, 11815–11824.

(62) Mohr, C.; Lopez-Hilfiker, F. D.; Zotter, P.; Prevot, A. S.; Xu, L.; Ng, N. L.; Herndon, S. C.; Williams, L. R.; Franklin, J. P.; Zahniser, M. S.; Worsnop, D. R.; Knighton, W. B.; Aiken, A. C.; Gorkowski, K. J.; Dubey, M. K.; Allan, J. D.; Thornton, J. A. Contribution of nitrated phenols to wood burning brown carbon light absorption in Detling, UK during winter time. *Environ. Sci. Technol.* **2013**, *47*, 6316–6324.

(63) Teich, M.; van Pinxteren, D.; Wang, M.; Kecorius, S.; Wang, Z.; Müller, T.; Mocnik, G.; Herrmann, H. Contributions of nitrated aromatic compounds to the light absorption of water-soluble and particulate brown carbon in different atmospheric environments in Germany and China. *Atmos. Chem. Phys.* **2017**, *17*, 1653–1672.

(64) Desyatnik, Y.; Sun, Y.; Shen, X.; Lee, T.; Wang, X.; Wang, T.; Collett, J. L. Speciation of brown carbon in cloud water impacted by agricultural biomass burning in eastern China. *J. Geophys. Res. Atmos.* **2013**, *118*, 7389–7399.

(65) Jo, D. S.; Park, R. J.; Lee, S.; Kim, S. W.; Zhang, X. A global simulation of brown carbon: implications for photochemistry and direct radiative effect. *Atmos. Chem. Phys.* **2016**, *16*, 3413–3432.

(66) Hammer, M. S.; Martin, R. V.; van Donkelaar, A.; Buchard, V.; Torres, O.; Ridley, D. A.; Spurr, R. J. D. Interpreting the ultraviolet aerosol index observed with the OMI satellite instrument to understand absorption by organic aerosols: implications for atmospheric oxidation and direct radiative effects. *Atmos. Chem. Phys.* **2016**, *16*, 2507–2523.